Desalination and Water Treatment
www.deswater.com

doi: 10.5004/dwt.2017.20774

85 (2017) 55–62
August

Prediction of water aeration efficiency in high turbulent flow

Florentina Bunea[a], Adrian Nedelcu[a,*], Dan Gabriel Ciocan[b]

[a]*National Institute for Research and Development in Electrical Engineering ICPE-CA, Efficiency in Conversion and Consumption of Energy Department, 313 Splaiul Unirii, 030138 Bucharest, Romania, Tel. +40723121544; emails: adrian.nedelcu@icpe-ca.ro (A. Nedelcu), florentina.bunea@icpe-ca.ro (F. Bunea)*
[b]*Pavillon Adrien-Pouliot Université Laval, Laboratoire de Machines Hydrauliques, 1065 Rue de la médecine, Québec, Canada G1V 0A6, email: gabrieldan.ciocan@orange.fr*

Received 5 October 2016; Accepted 26 March 2017

ABSTRACT

This paper presents the study of a complex turbulent flow with disperse gas–liquid flow with adverse pressure gradient, where the mass transfer through the interface is a dynamic process associated with the interface' dynamics, and the interface's aria varies along the flow. The experimental setup is equipped with a disperse aeration device, fitted with interchangeable perforated plate. The air flow is injected as disperse bubbles of different sizes at different air flow rates through the performed plates. This paper presents the aeration performances of four disperse aeration devices, mounted non-invasive on the wall of a pipeline. The water flow corresponds to Reynolds number in the range 1×10^5 to 5×10^5. The objective is to find the optimal aeration device to increase the transfer of the dissolved oxygen content in water, with a minimum power and volume of injected air. The following parameters are considered: the dissolved oxygen deficit from the water, the air–water interface area, pressure losses of the aerator, aerator design and the contact time of the two phases. The aeration devices are tested for different void fraction and the following parameters are obtained: volumetric mass transfer, standard oxygen transfer rate, standard oxygen transfer efficiency, power consumption for air injection and standard aeration efficiency. Finally, a comparative study on the *kLa* performance of several types of aerators is presented.

Keywords: Air injection; Disperse aeration device; Aerator; Dissolved oxygen; Oxygen transfer; Rotational biphasic flow; Turbine aeration

1. Introduction

The paper presents a laboratory study of some non-invasive aeration devices to be mounted on the draft tube of hydraulic turbines, which equip the hydropower plants (HPPs) to mitigate the dissolved oxygen (DO) deficit from turbined water. The actual aeration solutions applied to hydraulic turbines improve the DO level with an associated loss of the hydraulic efficiency [1–3] due to the internal flow modification. Currently there is no general efficient method for aeration of water passing through hydraulic turbines. Each implementation requires customized studies and a custom solution for every turbine. In literature can be found many investigations related to the air transfer in water column [4], but no fundamental studies were performed in turbulent flow with adverse pressure gradient. The aeration efficiency of auto-venting turbines, in term of oxygen transfer, is analyzed and compared in literature [2,3,5,6], based on site measurements, highlighting the main parameters of aeration: turbine geometry, air quantity, air intake, etc.

In general, to increase the DO level with 1 mg/L the air quantity required is of 1% of transited water volume [3,7]. On the other hand, to avoid a significantly decrease of the hydraulic efficiency, the air flow rate must be <3% of the turbined water flow rate (Eq. (1)). Actual methods of turbines water aeration affect the efficiency of the HPP due to the flow perturbations by introduction of the air, as well as by the

* Corresponding author.

electrical power consumption to inject the air (e.g., compressor station).

$$Q_{air} < (1 \div 3\%) Q_{water} \quad (1)$$

This is a current problem of manufacturer and operators of hydraulics turbines, therefore, the air injection (the method, intake, quantity, etc.) becomes an important parameter to the balance between turbine efficiency and ecological factor.

Aeration of the hydraulic turbine is usually expressed by the void fraction:

$$\phi = \frac{Q_{air}}{Q_{water}} \cdot 100[\%] \quad (2)$$

where Q_{air} and Q_{water} are the air flow rate and, respectively, the water flow rate.

This paper presents an experimental approach to define the best aerations parameters to be implemented in a hydraulic turbine. The experimental setup is designed to reproduce the flow features in a hydraulic turbine draft tube. The design of a specific test bench, the measurement performed and the analysis of the results are presented. The standard aeration efficiency (SAE) is finally obtained for four aeration devices. The results are compared with other literature results for aeration systems.

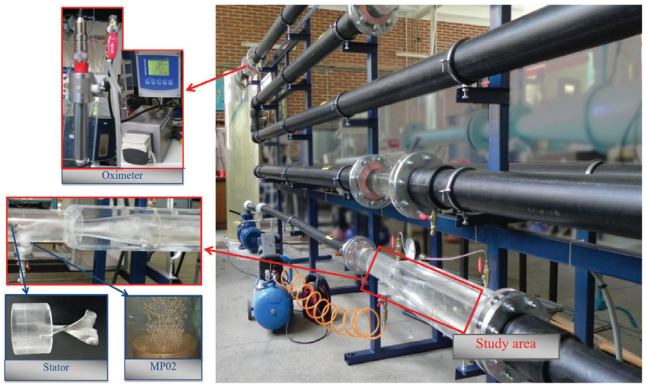

Fig. 1. Test bench for study of rotational biphasic flow with adverse pressure gradient.

2. Experimental setup

A test bench was designed to reproduce the rotational, biphasic flow with adverse pressure gradient [8]. It is a closed-loop setup (Fig. 1), that consists from a water still tank from which the water is pumped into a pipe of 50 mm diameter. The adverse pressure gradient effect (divergent effect) is obtained using a conic shape with a flaring angle $\gamma = 7°$, which is correlated with flaring angle of turbine draft tube (γ = 0°...12°). Upstream of the conic section there is a stator with the purpose to induce the rotational flow. With the increase the water velocity, the rotational flow induced by the stator develops a vortex that can become cavitational [9] (Fig. 2).

An aerator, placed downstream the stator and upstream the divergent section, is mounted non-invasive on the wall of the pipe so that the hydraulic circuit is not perturbed. The aerator has interchangeable perforated metallic plates (MP) for disperse aeration, each plate having a different holes diameter to allow variation of water–air interface area. The characteristics of tested MP are presented in Table 1. The holes are distributed at a distance of 6*d* in order to avoid bubble coalescence, and depth of the hole is 5*d*, to neglect the contraction coefficient of the hole. For a fair comparison between the results, the air emission area (the product of hole area and number of holes) through MP is the same for all the plates.

The hydraulic circuit is designed to consider the medium time for a bubble to travel from inlet to outlet of the Francis turbine's draft tube (min 10 s) with an average water velocity of 3 m/s. Therefore, the hydraulic circuit is continued with a 30 m long pipeline of 100 mm diameter before the water is evacuated back into the water stilling tank. The test bench has also measurement instrumentation such as: flowmeter for water flow rate, rotameter for air flow rate, oximeter for DO and pressure sensors, etc. (Fig. 3).

Table 1
Characteristics of tested MP

MP characteristics	MP01	MP02	MP03	MP05
Air emission area (mm^2)	29.88	29.86	29.88	29.83
Hole diameter, *d* (mm)	0.1	0.2	0.3	0.5
Distance between holes (mm)	0.6	1.2	1.8	3

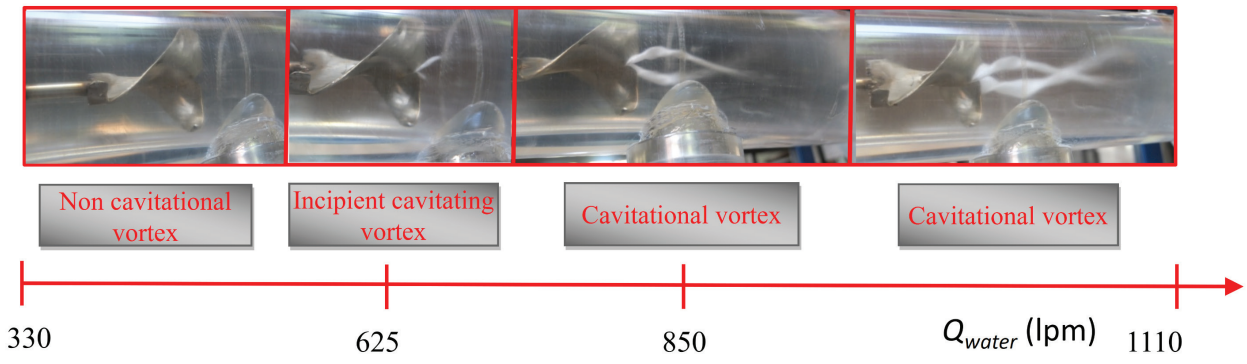

Fig. 2. Rotational flow induced by stator and vortex development stages.

The procedure for mass transfer evaluation for each set point consists of:

- Deaeration of the water, using for example sodium sulphite, to a DO concentration <0.3 mg/L;
- Setting the water flow rate and stabilization of the flow;
- Setting the injected air flow rate, knowing the pressure levels in the critical points of study area;
- Acquisition of the DO concentration in time, considering the water and air temperatures, for the defined parameters (air and water flow rates); the water is aerated until 90% of saturation according to ASCE 2-91/1993 [10] and
- Numerical processing of the acquired data to determine the aeration efficiency for the set point.

3. Experimental evaluation of DO transfer in turbulent flows

To determine the aeration efficiency, it is necessary to estimate the pressure loss on metallic plates of the aerator. As such the experimental configuration from Fig. 3 was used for its measurement. In Fig. 4, the variation of the pressure loss function of injected air flow rate for all MP is presented. It can be observed how the pressure loss decreases with the increase of MP holes' diameter.

DO content evaluation is done by sampling the water from downstream of experimental setup using a peristaltic pump and an oximeter (Fig. 1). Samples are returned into main flow by the same pump. A total of 28 cases of $C = f(t)$ were investigated at the injected air flow rates between 5 and 12 lpm and the water flow rates between 330 and 1,110 lpm, according to the set points from Table 2. The measurements were performed in steady stabilized conditions for the void fractions ϕ showed in Table 2. The $\phi \leq 1.5\%$ is imposed, according to Eqs. (1) and (2).

Depending on the time until 90% of DO saturation concentration was reached, 140...760 samples were taken for each set point. After each measurement run, the procedure [10] is repeated for another set point from DO removal until at least 90% from DO saturation concentration.

3.1. Experimental data processing and analysis

The procedure to estimate the volumetric oxygen transfer coefficient, *kLa*, and the DO saturation concentration at work temperature, C_s [1], applied for MP02 at set point Q_{air} = 8 lpm and Q_{water} = 1,110 lpm (ϕ = 0.72%) is presented in this paragraph.

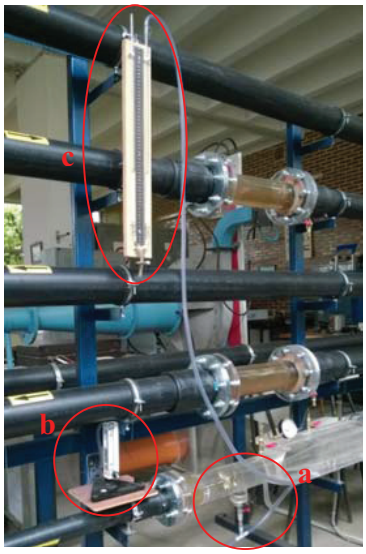

Fig. 3. Configuration for measurement of the pressure loss on MP (a – aerator, b – rotameter and c – differential manometer).

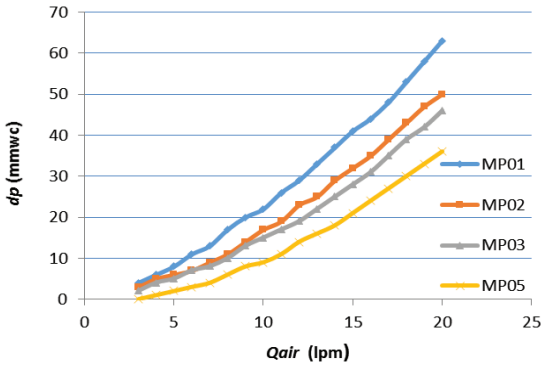

Fig. 4. The pressure loss related to the injected air flow rate for each MP.

Table 2
Void fraction (%) for tested MPs

Q_{water} (lpm)	MP01				MP02				MP03				MP05				Observed
	Q_{air} (lpm)				Q_{air} (lpm)				Q_{air} (lpm)				Q_{air} (lpm)				
	5	8	10	12	5	8	10	12	5	8	10	12	5	8.5	10	12	
330	1.51				1.51				1.51				1.51				Non-cavitational vortex
882	0.57				0.57				0.57				0.57				Incipient cavitational vortex
1,044	0.48				0.48				0.48				0.48				Developed cavitational vortex
1,110	0.45	0.7	0.9	1.1	0.45	0.72	0.9	1.1	0.45	0.72	0.9	1.1	0.45	0.72	0.9	1.1	Developed cavitational vortex

The concentration curve vs. time, $C = f(t)$, is plotted with data recorded from experimental run (Fig. 5). Considering the DO saturation content C_w [11], the DO relative content, C_{rel}, is obtained for each sample, according to $C_{rel} = C \times 100/C'_w$ (%), where C'_w is nearest neighbour interpolation of C_w at work temperature.

The DO content adjusted for 20°C is calculated by using the relation $C_{20} = C_{rel} \times C_{w20}$ (mg/L), where $C_{w20} = 9.19$ mg/L [11].

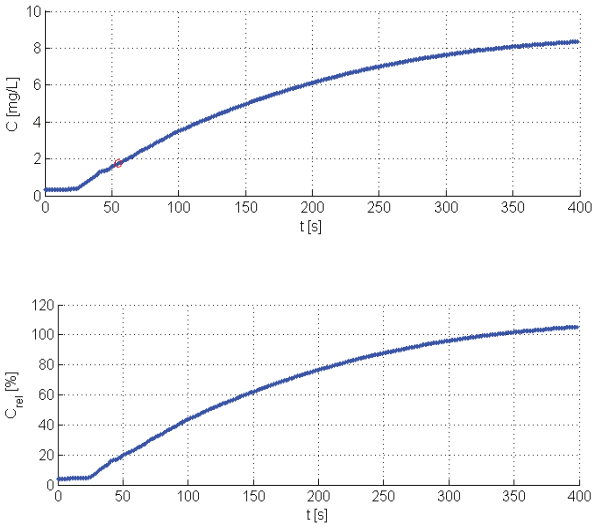

Fig. 5. Plotting of $C = f(t)$ and $C_{rel} = f(t)$ using experimental data and detection of inflexion point.

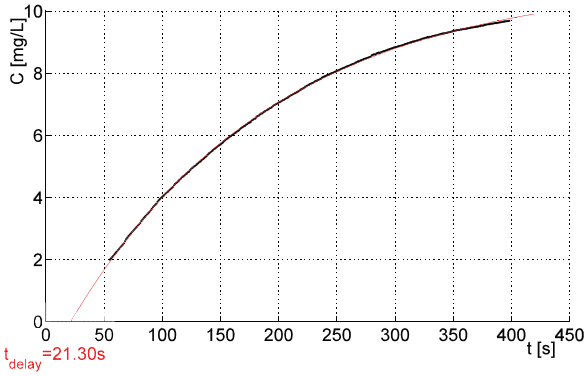

Fig. 6. Extrapolation of experimental data to obtain the delay time for MP02, Q_{air} = 8 lpm, Q_{water} = 1,110 lpm (black – experimental data and red – fitted curve).

The values less of 20% of saturation concentration because it is an inflexion point of the concentration curve (Fig. 5) are removed [10]. Eq. (3) is used to extrapolate the curve to the point $C = 0$, which gives the delay time, t_{delay}. The curve is then translated by subtracting the obtained delay time, such that at $t = 0$, the concentration $C = 0$ (Fig. 6).

$$C(t) = C_S - \left(C_S - C_0\right)e^{-kLa \cdot t} \tag{3}$$

where C is the concentration of DO at t seconds, C_0 is the oxygen concentration at $t = 0$, kLa (1/s) is the volumetric oxygen transfer coefficient and C_s (mg/L) is the DO saturation concentration at work temperature.

The corrected data are fitted using the same mathematical model as in the standard and given by Eq. (3), where $C_0 = 0$ (Fig. 7). This produces the values for kLa (1/min) and C_s (mg/L) parameters, for the current set point.

The algorithm is repeated for all 28 measurement points. In Table 3 and Figs. 8–10 are presented the variation of volumetric coefficient of mass transfer for all tested cases.

Standard oxygen transfer rate (SOTR), also known as oxygenation capacity, is calculated with Eq. (4) for each MP:

$$\text{SOTR} = kLa \cdot C_s \cdot V(mg/\text{min}) \tag{4}$$

where V = 534 L is the water volume in the experimental setup.

In Table 4 and Figs. 11–13 variation of the SOTRs function of different parameters for all set points and MPs are presented.

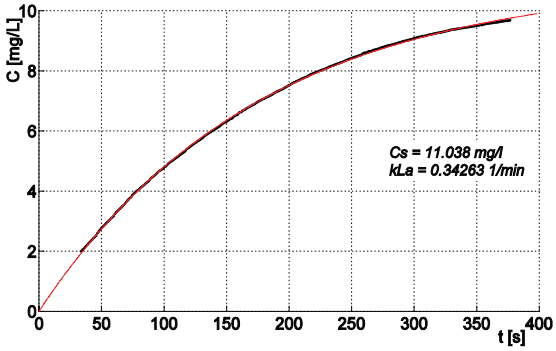

Fig. 7. Estimation of kLa and C_s parameters through non-linear regression for MP02, Q_{air} = 8 lpm, Q_{water} = 1,110 lpm.

Table 3
kLa (1/min) function of water and air flow rates

Q_{water} (lpm)	MP01				MP02				MP03				MP05			
	Q_{air} (lpm)				Q_{air} (lpm)				Q_{air} (lpm)				Q_{air} (lpm)			
	5	8	10	12	5	8	10	12	5	8	10	12	5	8.5	10	12
330	0.071				0.084				0.068				0.079			
882	0.184				0.195				0.173				0.188			
1,044	0.202				0.230				0.183				0.179			
1,110	0.200	0.32	0.380	0.496	0.223	0.343	0.382	0.469	0.196	0.322	0.364	0.404	0.193	0.340	0.338	0.386

Standard oxygen transfer efficiency (SOTE) is determined by Eq. (5):

$$\text{SOTE} = \frac{\text{SOTR}}{W_{O_2}}[-], \tag{5}$$

where SOTR is in kg/h and W_{O_2} is in kg/s – oxygen mass flow rate from the injected air. Considering that oxygen mass is 23% of total air mass:

$$W_{O_2} = 0.2765\, Q_s. \tag{6}$$

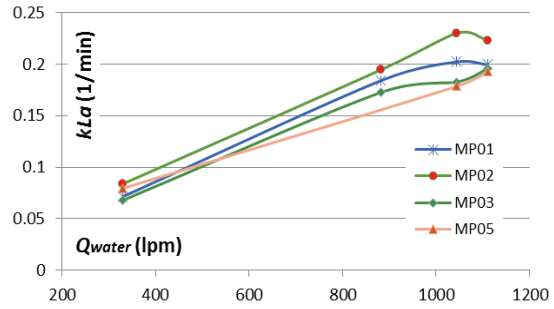

Fig. 8. *kLa* variation, for Q_{air} = 5 lpm = constant for different water flow rates.

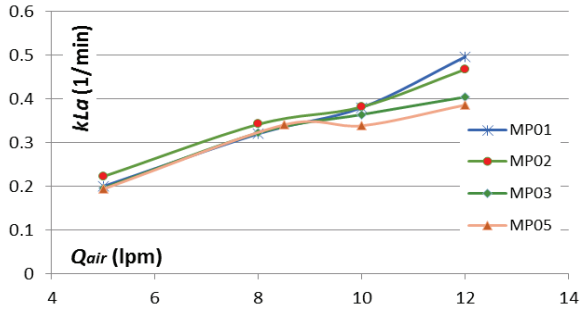

Fig. 9. *kLa* variation for Q_{water} = 1,110 lpm = constant for different air flow rates.

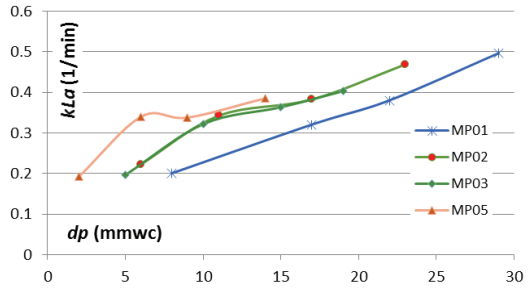

Fig. 10. *kLa* function of the pressure loss on tested MP.

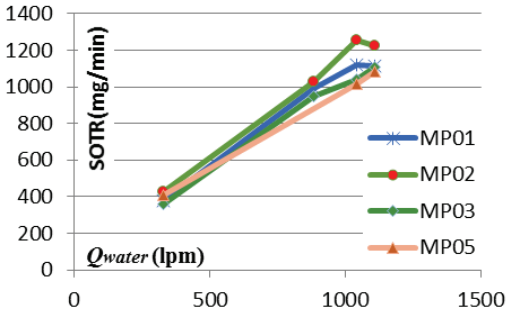

Fig. 11. SOTR variation at Q_{air} = 5 lpm = constant for different water flow rates.

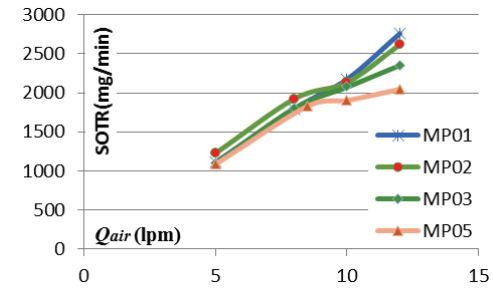

Fig. 12. SOTR variation at Q_{water} = 1,110 lpm = constant for different air flow rates.

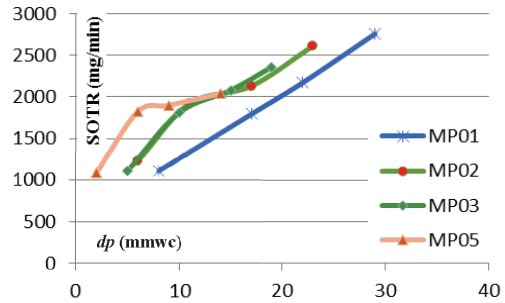

Fig. 13. SOTR function of pressure loss for tested MPs.

Table 4
SOTR (mg/min) variation with water and air flow rate

Q_{water} (lpm)	MP01				MP02				MP03				MP05			
	Q_{air} (lpm)				Q_{air} (lpm)				Q_{air} (lpm)				Q_{air} (lpm)			
	5	8	10	12	5	8	10	12	5	8	10	12	5	8.5	10	12
330	377				428				357				408			
882	992				1,030				949				1,017			
1,044	1,117				1,255				1,043				1,018			
1,110	1,112	1,797	2,176	2,759	1,225	1,921	2,131	2,616	1,105	1,809	2,079	2,358	1,083	1,826	1,899	2,041

Table 5
SAE (kg_{OD}/kWh) dependency of air and water flow rate

Q_{water} (lpm)	MP01				MP02				MP03				MP05			
	Q_{air} (lpm)				Q_{air} (lpm)				Q_{air} (lpm)				Q_{air} (lpm)			
	5	8	10	12	5	8	10	12	5	8	10	12	5	8.5	10	12
330	18,72				21,3				17,78				20,33			
882	49,27				51,2				47,25				50,70			
1044	55,48				62,4				51,91				50,77			
1110	55,22	55,5	53,54	56,32	61,0	59,53	52,62	53,60	54,99	56,10	51,39	48,44	54,01	56,78	47,14	42,07

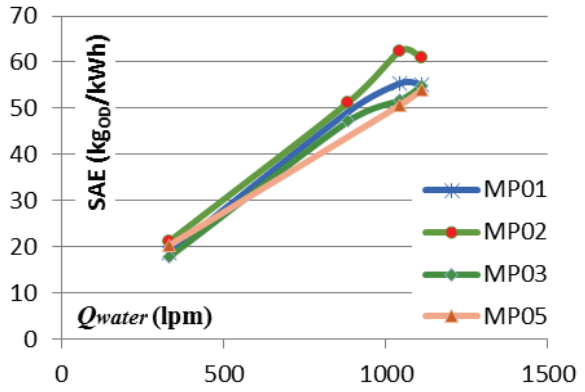

Fig. 14. SAE variation at Q_{air} = 5 lpm = constant for different water flow rates.

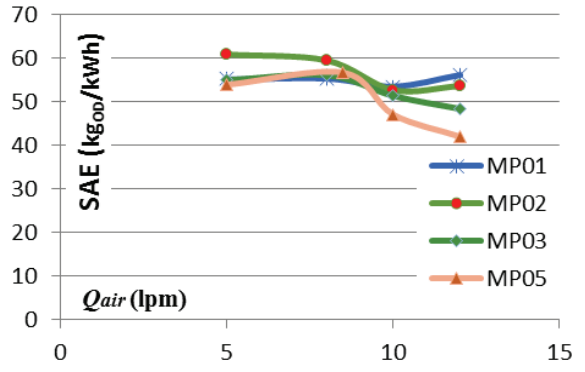

Fig. 15. SAE variation at Q_{water} = 1,110 lpm = constant for different air flow rates.

$$Q_s = \frac{Q \cdot 273.15}{273.15 + \theta} \left[\mathrm{m^3/s}\right] \tag{7}$$

then the air flow rate adjusted to standard conditions, where θ is the air temperature in °C. Finally, the SAE is determined using Eq. (8):

$$\mathrm{SAE} = \frac{\mathrm{SOTR}}{P} \left[\mathrm{kg_{OD}/kWh}\right], \tag{8}$$

where P is the power consumption for air injection through MP (Eq. (9)), considering the hydrostatic load on the plate

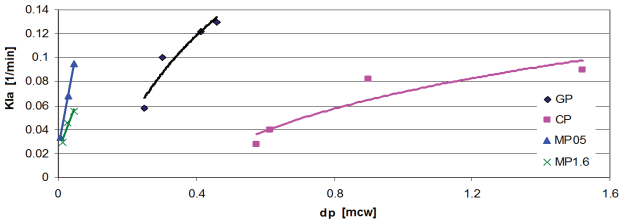

Fig. 16. $kLa = f(dp)$ for several aerator plates.

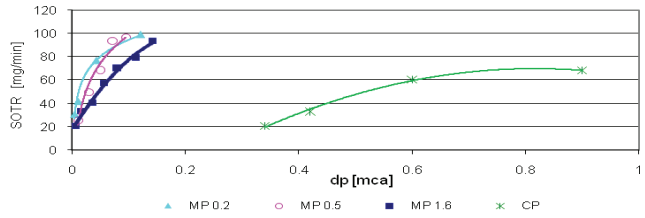

Fig. 17. Standard oxygen transfer rate function of pressure loss on different types of aerator plates.

$H \approx 1.47$ mwc and dp the pressure loss of MP expressed in Pa, experimentally obtained (Fig. 4).

$$P = Q_{water}(dp + \rho g H)/1000 \left[\mathrm{kW}\right] \tag{9}$$

The results are presented in Table 5 and Figs. 14 and 15.

Figs. 16 and 17 are represented the experimental results, processed to obtain the main parameters which characterize the aeration process in standard conditions.

Analyzing the experimental results on the correlation between holes' diameter and DO level in rotational flows is observed that the most efficient plate is MP02. This is noticeable on *kLa*, SOTR, SOTE and SAE plots where the curve of MP01 is slightly below MP02. The very fine holes of MP01 clogged during the measurement and the effective area of injection decreased for MP01.

4. Results and discussion

In order to select an MP with the best ratio between aeration capacity and pressure loss is presented in the following a comparative study between several aeration plates. The tested plates in this paper were chosen based on previous research on several types of aeration devices [12–14],

while their typo-dimensions must be adapted to the specific application. Many advanced theoretical and applied researches concerning the hydro-gas-dynamics of the fine bubbles columns are performed in order to improve the efficiency of the mass transfer and to diminish the operation costs [15–18]. High efficiency aeration devices and operation control strategy are studied in [19] in order to improve the energy consumption of wastewater treatment plants.

In a continuous attempt to improve aeration performances, different types of aerators are developed, made from ceramic or plastic materials, perforated rubber, etc. and having various porosities and shapes [20,21]. For accomplishing an efficient aeration, the aerators must provide fine bubbles to increase the interface contact area.

Figs. 16 and 17 present comparative experiments done in a still water tank for several types of aeration plates: a sintered glass plate with porosity of 0.1–0.25 mm, a ceramic plate with volumetric porosity of 40%–50% and three perforated metallic plates with holes of 0.2, 0.5 and 1.6 mm (MP02, MP05 and MP1.6). It is observed that the aeration performance of perforated plates is comparable with the others but with a higher reduction of pressure loss, which is leading to superior efficiency of aeration. In case of rotational flow with cavitational vortex there is no hydrostatic load on the MP, so there is no risk of water infiltrating the aerator, perforated plates are favoured because of their low power consumption for air injection which leads to a high efficiency.

5. Conclusions

The aim of the paper is to study and optimize the disperse aeration solutions in turbulent flows corresponding with hydraulic turbines flow: the flow parameters are similar with the draft tube of hydraulic turbines flow. The injected air volume into the hydraulic system, corresponds to a void fraction $\phi \leq 1\%–3\%$ to reduce the impact of the air flow injection on the flow structure and consequently on the hydraulic efficiency of the turbine.

The experimental setup is designed for laboratory study of high turbulent flows, with regard to flow parameters in the draft tube of a hydraulic turbine, i.e., the adverse pressure gradient, mean water velocity, time of air–water contact, rotational flow with cavitational vortex. This allows visualization of the emergence and development of cavitational vortex.

In order to select the best aeration performance suitable in high turbulent flow which develops a cavitational vortex in various evolution stages, four aerators with perforated plates were tested, with a different hole's diameter, mounted non-invasive on the wall of the pipe. For the comparison of the results, the air emission surface was chosen equal for all MPs. Thus, the four aerators were characterized in flows with different turbulent stages (mean water velocities from 2.5 to 9 m/s), at different injected air flow rates, in order to cover a void fraction in the range 0.45%–1.5%.

The following parameters were computed based on experimental data: the volumetric mass transfer, SOTR, SOTE, power consumption for air injection and finally the SAE.

Experimental research regarding mass transfer conducted for several MP types underlined that the increase of air flow rate leads to the increase of the volumetric mass transfer coefficient, *kLa*, but at high values of the flow rate, *kLa* shows a flattening trend, which is confirmed by literature. This experimental research quantifies the aeration efficiency vs. aeration parameters, flow characteristics and practical limitations (clogging). The flow is similar to the cavitating flow from turbine draft tube. The optimal solution of aeration, specific of this application, was obtained and the results are compared with literature results.

Acknowledgement

The work has been funded by the Executive Agency for Higher Education, Research, Development and Innovation (UEFISCDI), PN-II-PT-PCCA-2013-4 program, ctr. no. 88/2014, ECOTURB project.

Symbols

C_{rel}	—	DO relative content, mg/L
C_s	—	Saturation concentration of dissolved oxygen at work temperature, mg/L
$C(t)$	—	Concentration of dissolved oxygen at t seconds, mg/L
C_w	—	DO saturation content, mg/L
C'_w	—	Nearest neighbour interpolation of C_w at work temperature, mg/L
C_{w20}	—	DO saturation content at 20°C, mg/L
C_0	—	Concentration of dissolved oxygen at t = 0, mg/L
C_{20}	—	DO content adjusted at 20°C, mg/L
d	—	Hole diameter, mm
dp	—	Pressure loss of MP, mmwc
g	—	Gravitational acceleration, m/s^2
H	—	Hydrostatic load, mwc
kLa	—	Volumetric oxygen transfer coefficient, 1/s
P	—	Power consumption for air injection, kW
Q_{air}	—	Air flow rate, lpm
Q_s	—	Air flow rate adjusted to standard conditions, m^3/s
Q_{water}	—	Water flow rate, lpm
SAE	—	Standard aeration efficiency, kg_{OD}/kWh
SOTR	—	Standard oxygen transfer rate, mg/min
SOTE	—	Standard oxygen transfer efficiency
t_{delay}	—	Delay time, s
V	—	Water volume, L
W_{O_2}	—	Oxygen mass flow rate from the injected air, kg/s
γ	—	Flaring angle, °
θ	—	Air temperature, °C
ρ	—	Water density, kg/m^3
ϕ	—	Void fraction, %
DO	—	Dissolved oxygen
MP	—	Perforated metallic plate
MP01	—	Metallic plate perforated with holes of 0.1 mm diameter
MP02	—	Metallic plate perforated with holes of 0.2 mm diameter
MP03	—	Metallic plate perforated with holes of 0.3 mm diameter
MP05	—	Metallic plate perforated with holes of 0.5 mm diameter

References

[1] F. Bunea, G.D. Ciocan, A. Nedelcu, D.M. Bucur, G. Dunca, R. Chihaia, Experimental setup for the study of new aeration devices in hydraulic turbines, Environ. Eng. Manage. J., 16 (2017) 1033–1040.

[2] F. Bunea, G.D. Ciocan, G. Oprina, G. Băran, C.A. Băbuțanu, Hydropower impact on water quality, Environ. Eng. Manage. J., 9 (2010) 1459–1464.

[3] D.C. Raney, T.G. Arnold, Dissolved oxygen improvement by hydroelectric turbine aspiration, J. Power Div., 99 (1973) 139–152.

[4] M. Motarjemi, G.J. Jameson, Mass transfer from very small bubbles: the optimum bubble size for aeration, Chem. Eng. Sci., 33 (1978) 1415–1423.

[5] B. Papillon, M. Sabourin, M. Couston, C. Deschenes, Methods for Air Admission in Hydroturbines, XXIst IAHR Symposium on Hydraulic Machinery and Systems, Lausanne, 2002.

[6] A. Sullivan, K. Bennet, Retrofit Aeration System (RAS) for Francis Turbine, Final Report, Ameren UE and MEC Water Resources Inc., Contract FC36-02ID14408, US, 2006.

[7] P.A. March, T.A. Brice, M.H. Mobley, J.M. Cybularz, Turbines for solving the DO dilemma, Hydro Rev., 11 (1992) 30–36.

[8] F. Bunea, G.D. Ciocan, Test Bench for Study of Rotational Biphasic Flow Study with Adverse Pressure Gradient, Patent Application Registration, OSIM No. A/00704/29.09.2015, 2015.

[9] A. Digulescu, I. Murgan, F. Bunea, G.D. Ciocan, DM. Bucur, G. Dunca, I. Candel, C. Ioana, Cavitating vortex characterization based on acoustic signal detection, IOP Conf. Ser.: Earth Environ. Sci., 49 (2016) 082009.

[10] ANSI/ASCE, Measurement of Oxygen Transfer in Clean Water, 2nd ed., Standard No. 2-91/1993, American Society of Civil Engineers, 1993, p. 45.

[11] Winkler Titration, Standard Operating Procedure for Dissolved Oxygen Micro Method, 2007. Available at: http://www.epa.gov/greatlakes/monitoring/sop/chapter_5/LG501.pdf

[12] F. Bunea, G.D. Ciocan, D.M. Bucur, G. Dunca, Aeration Solution of Water Used by Hydraulic Turbines to Respect the Environmental Policies, International Conference and Exposition on Electrical and Power Engineering, IEEE, 2014, pp. 1015–1020.

[13] F. Bunea, G. Oprina, G.D. Ciocan, G. Băran, C. Ilie, I. Pincovschi, Aeration parameters optimization for an imposed energy consumption, Appl. Math. Mech., 2 (2009) 279–284.

[14] I. Murgan, F. Bunea, G.D. Ciocan, Experimental PIV and LIF characterization of a bubble column flow, Flow Meas. Instrum., 54 (2017) 224–235. Available at: http://dx.doi.org/10.1016/j.flowmeasinst.2017.02.004

[15] M. Jamnongwong, T. Charoenpittaya, N. Hongprasith, T. Imai, P. Painmanakul, Study of liquid film forming apparatus (LFFA) mechanisms in terms of oxygen transfer and bubble hydrodynamic parameters, Eng. J., 20 (2016) 77–90.

[16] A. Zaruba, E. Krepper, H.M. Prasser, B.N. Reddy Vanga, Experimental study on bubble motion in a rectangular bubble column using high-speed video observations, Flow Meas. Instrum., 16 (2005) 277–287.

[17] A.V. Kulkarni, J.B. Joshi, Design and selection of sparger for bubble column reactor. Part I: performance of different spargers, Chem. Eng. Res. Des., 89 (2011) 1972–1985.

[18] C. Liu, S. Li, F. Zhang, The oxygen transfer efficiency and economic cost analysis of aeration system in municipal wastewater treatment plant, Energy Procedia, 5 (2011) 2437–2443.

[19] H. Fan, L. Qi, Y. Zhang, Q. Fan, H. Wang, Aeration optimization through operation at low dissolved oxygen concentrations: evaluation of oxygen mass transfer dynamics in different activated sludge systems, J. Environ. Sci., 55 (2017) 224–235. Available at: http://dx.doi.org/10.1016/j.jes.2016.08.008

[20] M. Gafsi, A. Kettab, A. Djehiche, K. Goteicha, Study of the efficiency of hypolimnetic aeration process on the preservation of the thermal stratification, Desal. Wat. Treat., 57 (2016) 6017–6023.

[21] M. Bodzek, K. Konieczny, A. Kwiecińska, Application of membrane processes in drinking water treatment–state of art, Desal. Wat. Treat., 35 (2011) 164–184.